

Electrical and Magnetoresistive studies Nd doped on La-Ba-Mn-O₃ Manganites for Low-field Sensor application

¹H. Abdullah and ²S.A. Halim

¹Department of Electrical, Electronic and System Engineering,
Faculty of Engineering and Built Environment,
Universiti Kebangsaan Malaysia, 43600 UKM Bangi, Malaysia

²Superconductor and Thin Films Laboratory, Department of Physics,
Faculty of Science and Environmental, University Putra Malaysia, 43400 Serdang, Selangor, Malaysia

Abstract: Problem statement: Electrical and magnetoresistive properties of the Nd doped (La_{1-x}Nd_x)_{0.5}Ba_{0.5}MnO₃ type samples with $0 \leq x \leq 1.0$ had been prepared using the solid state reaction. These materials are extensively studied by the substitution of rare-earth compound is to understand the nature of transport phenomena in each system. **Approach:** The samples were calcined at 900°C for 12 h, pelletized and sintered at 1300°C for 24 h. Electrical property had been determined by using standard four-point probe resistivity measurement within a temperature range of 30-300 K. The Magnetoresistance (MR) was measured using a conventional four terminal method with magnetic fields of $H \leq 1$ T at 90, 100, 150, 200, 250, 270 and 300 K. **Results:** The metal-insulator transition temperature, T_p shifted towards lower temperatures as Nd doping increased followed by decreasing of the activation energy (E_a). The observed behavior had been explained on the basis of oxygen deficiency present in the samples. The electrical resistivity data were analyzed using various theoretical models and it had been concluded that the electrical resistivity data in the low temperature regime ($T < T_p$) can be explained using the equation $\rho = \rho_0 + \rho_2 T^2 + \rho_{4,5} T^{4,5}$, signifying the importance of the grain/ domain boundary, electron-electron and two magnon scattering processes. On the other hand, the high-temperature resistivity data ($T > T_p$) were explained using variable range mechanism. All samples exhibit LFMR and HFMR regime, except $x = 1$ at higher temperature. Overall, MR drops slowly when temperature was increased. All doping concentration gives small variation in MR (~8.97-~63.49%). The highest MR value of 63.49% was observed at 150 K for the $x = 1$ sample. **Conclusion:** In this case, it showed that LFMR can be observed at a temperature 90 K. it provided a large variation of LFMR in range of ~100-~160% MR/Tesla. These values were very sensitive for low-field application and therefore it's also acceptable as a requirement for a sensing element.

Key words: Metal-insulator transition temperature (T_p), Variable Range Hopping (VRH), Magnetoresistance (MR), Low-Field MR (LFMR), Low-Field MR (HFMR)

INTRODUCTION

The discovery of colossal magnetoresistivity in mixed valent manganites has led to a resurgence of interest in this family of compounds. The general formula $Ln_{1-x}A_xMnO_3$ (Ln = Rare earth and A = Divalent alkaline earth cation) has created deal of interest because of their Colossal Magnetoresistance (CMR) behavior. Thus even at the insulating LaMnO₃ end, strong correlation, Hund's rule and Jahn Teller effect are important. On substituting trivalent La with a divalent ion such as Ca or Ba, one d electron is transferred out from Mn^{3+} to oxygen, so that La_{1-x}Ba_xMnO₃ for instance has a fraction (1-x) of the

Mn ions in the 3+state and fraction x in the 4+state. These systems have technological importance such as in sensor application and increasing data storage by increasing in sensitivity of hard disk drive read heads^[1]. A large low-field MR capacity component has also been observed in polycrystalline manganite samples, with a disruption in the crystalline order at the grain boundaries induces a local spin disorder^[2,3]. Using Grain Boundaries (GB's) to manipulate the magnetic behavior has been proven to be a simple method for enhancing the low-field sensitivity of these materials. Many of the observed effects are due to the strong connection between magnetism and the insulator to metal transition special to these systems.

Corresponding Author: H. Abdullah, Department of Electrical, Electronic and System Engineering, Faculty of Engineering and Built Environment, University Kebangsaan Malaysia, 43600 UKM Bangi, Malaysia

MATERIALS AND METHODS

(La_{1-x}Nd_x)_{0.5}Ba_{0.5}MnO₃, with x = 0, 1/6, 1/3, 1/2, 2/3, 5/6 and 1, were prepared via the conventional solid-state reaction method. A well-mixed stoichiometric mixture of La₂O₃, Nd₂O₃, BaCO₃, MnCO₃ for (La_{1-x}Nd_x)_{0.67}Ba_{0.33}MnO₃ of 99.9% purities were mixed and grinded for 2 h. The dried powders were heated at 900°C in air for 12 h. After calcinations, the black powdery mixture was reground, pelletized and sintered in air at 1300°C for 24 h.

The DC four probe methods with closed cycle helium refrigerator in the temperature range of 30-300 K was used to investigate the electrical properties. The Magnetoresistance (MR) effects were studied by using the four point probe technique with magnetic fields of H≤1T at 90, 100, 150, 200, 250, 270 and 300 K.

RESULTS AND DISCUSSION

Electrical resistivity: The resistivity, ρ, of the (La_{1-x}Nd_x)_{0.5}Ba_{0.5}MnO₃ at zero field is shown in Fig. 1. The resistance plot of undoped and doped samples shows Metal-Insulator Transition (MIT) at T_p. All samples show semiconducting transport behavior above T_p and metallic behavior below T_p. With increasing Nd doping, T_p shifted to lower temperatures, which are 254, 244, 218, 198, 146, 130 and 114 K for x = 0, 1/6, 1/3, 1/2, 2/3, 5/6 and 1, respectively.

At low temperature (T<T_p) the metallic behavior of the samples can be explained in terms of electron-magnon scattering of the carriers (Fig. 2). In this temperature regime, the resistivity data fit quite well with the following expression:

$$\rho = \rho_0 + \rho_2 T^2 + \rho_{4.5} T^{4.5} \tag{1}$$

where, ρ₀ corresponds to the resistivity arising due to domain, defect, grain boundary and domain walls. The ρ₂T² term appears as a result of electron-electron and electron-phonon scattering mechanism^[5] and the, ρ_{4.5}T^{4.5} term corresponds to the electron-magnon scattering^[6]. Thus, the spin scattering cannot be neglected in the low temperature (T<T_p) regime as the measured data can be best explained by electron-magnon scattering.

The best fitted parameters are shown in Table 1. It is noted that the values of ρ₀, ρ₂T² and ρ_{4.5}T^{4.5} increase with the increase of x. However, the decrease of temperature independent ρ₀ is more significant with x compared to that of ρ₂. As the concentration increases, the size of the domain boundary decreases and ρ₀ becomes larger.

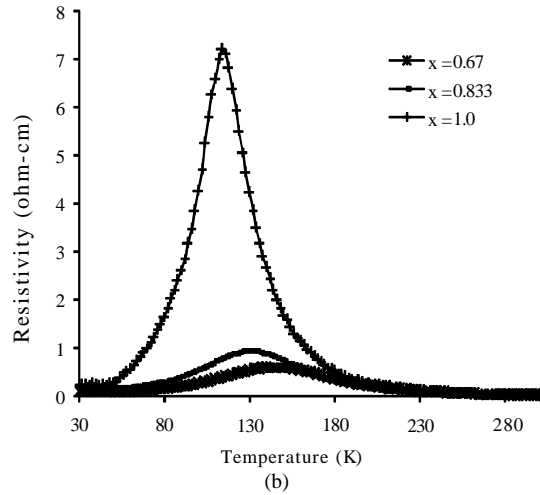
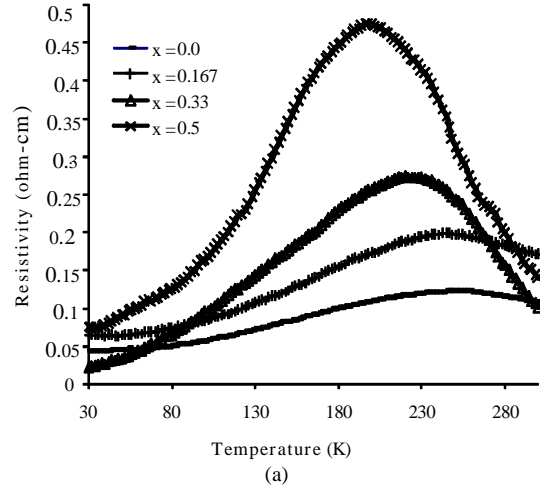


Fig. 1: The temperature dependence of the resistivity ρ(T) for the samples with x = 0, 1/6, 1/3, 1/2, 2/3, 5/6 and 1

Table 1: Best fitted parameters obtained from the fitting of the low temperature resistivity data in the metallic regime of (La_{1-x}Nd_x)_{0.5}Ba_{0.5}MnO₃ manganites with ρ = ρ₀+ρ₂T²+ρ_{4.5}T^{4.5}

Content, x	ρ ₀ (Ω cm)	ρ ₂ (Ω cm K ⁻²)	ρ _{4.5} (Ω cm K ^{-4.5})
0.000	0.042	1.50E-06	1.40E-12
0.167	0.060	2.40E-06	2.00E-12
0.330	0.018	7.00E-06	3.00E-12
0.500	0.065	1.00E-05	8.00E-12
0.670	0.080	4.00E-05	1.50E-10
0.833	0.140	1.30E-05	3.00E-10
1.000	0.200	4.00E-06	4.20E-09

The increment of ρ₂ and ρ_{4.5} with x is due to the suppression of spin fluctuation. Hence, the bandwidth (b_p) becomes smaller.

All resistivity data, above the transition temperature T_p, have been fitted with Variable Range

Hopping (VRH) model ($T_p < T < \theta_D/2$) of charge carriers where θ_D is debye Temperature. Sayani *et al.*^[4] applied VRH conduction mechanism in systems like $\text{La}_{1-x}\text{Ca}_x\text{K}_y\text{MnO}_3$. Our data between T_p and 300 K fit the VRH model quite well. The Mott's equation for VRH mechanism^[6] is given by:

$$\sigma = \sigma_0 \exp(-T_0/T)^{1/4} \quad (2)$$

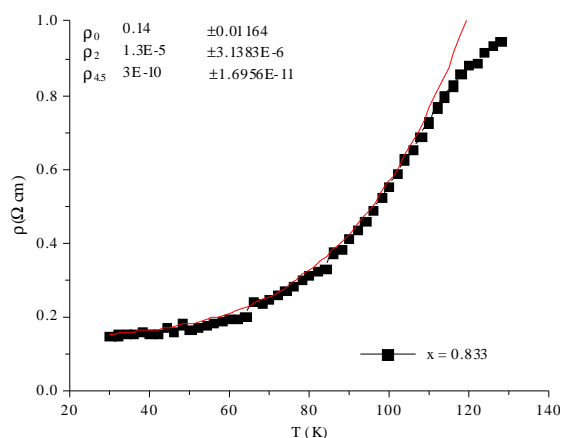
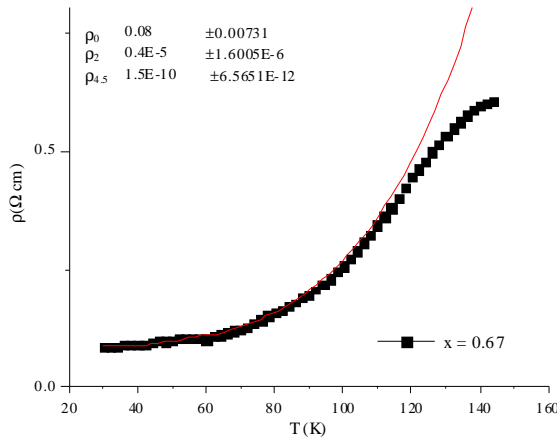
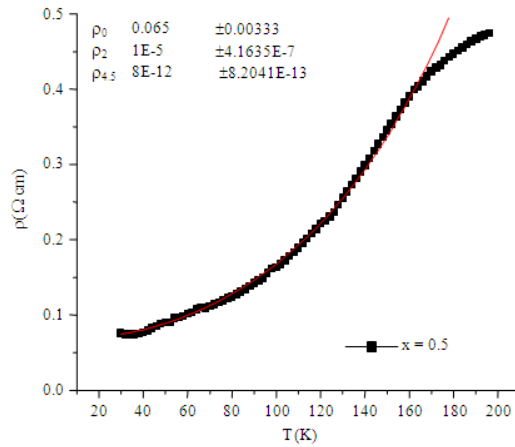
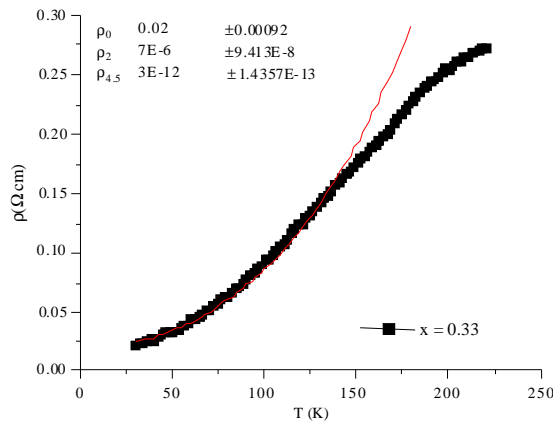
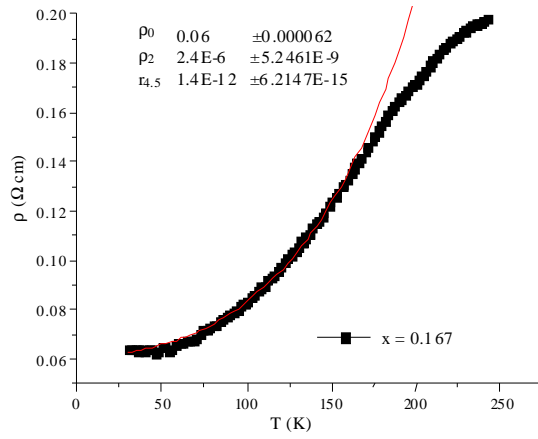
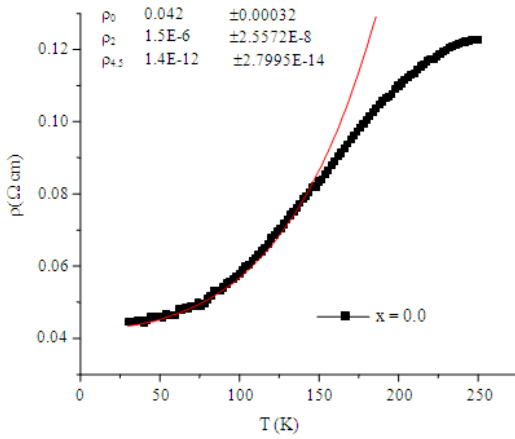
Where:

T_0 = A constant $[=18\alpha^3/k_B N(E_F)]$

α = The electron wave function decay constant

k_B = The Boltzmann's constant

$N(E_F)$ = The density of states at the Fermi level which can be calculated from the slope of the plot of $\log \sigma$ vs. $T^{-1/4}$ curves (Fig. 3)



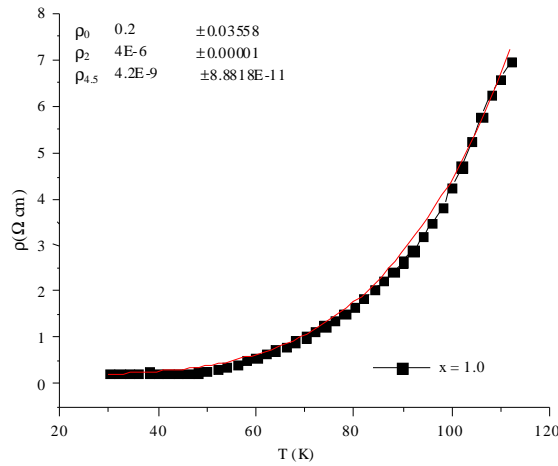


Fig. 2: Replotted resistivity data showing T^2 dependence for $(La_{1-x}Nd_x)_{0.5}Ba_{0.5}MnO_3$ with $x = 0, 1/6, 1/3, 1/2, 2/3, 5/6$ and 1 below the respective T_p . Solid lines are the best fit to the equation $\rho = \rho_0 + \rho_2 T^2 + \rho_{4.5} T^{4.5}$

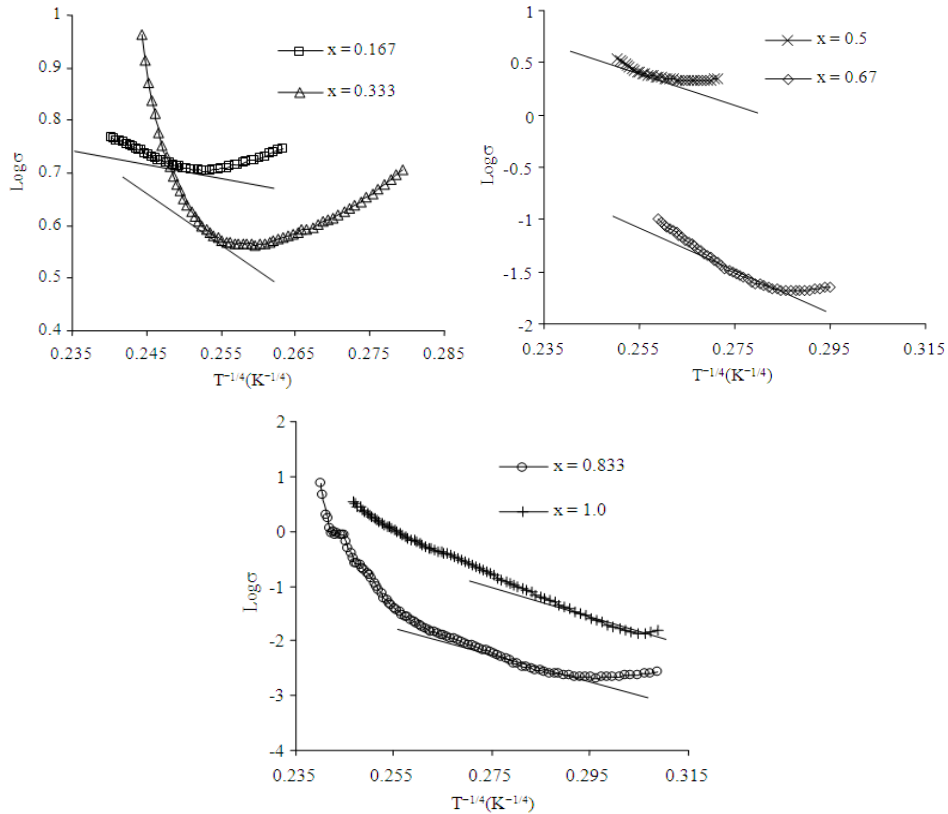


Fig. 3: The plot of $\log \sigma$ vs. $T^{-1/4}$ curves

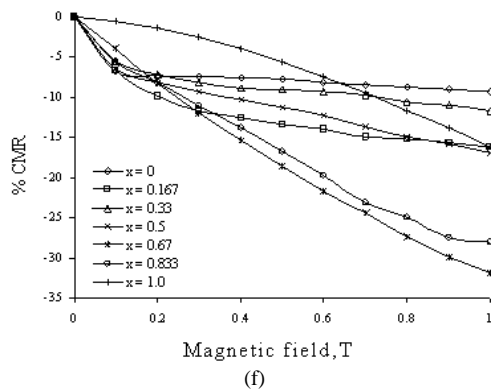
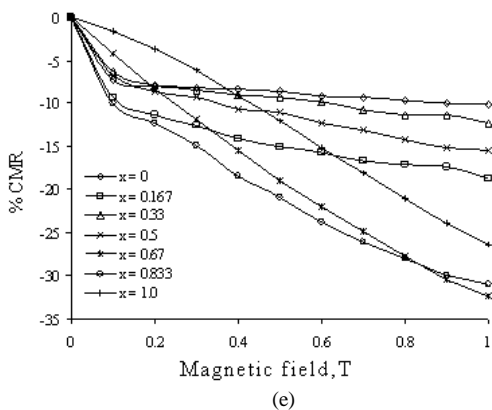
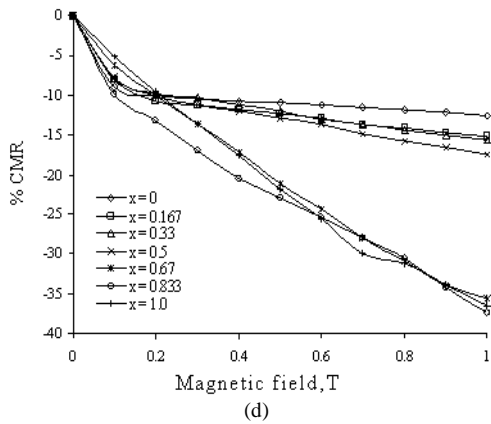
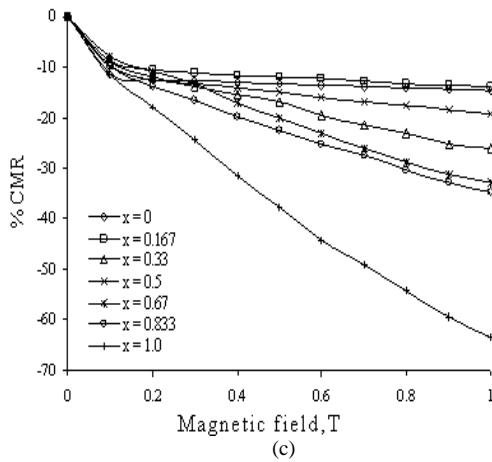
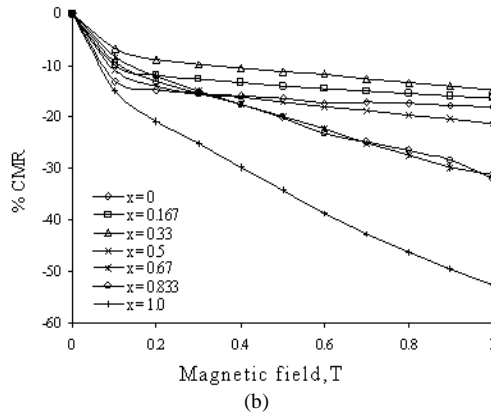
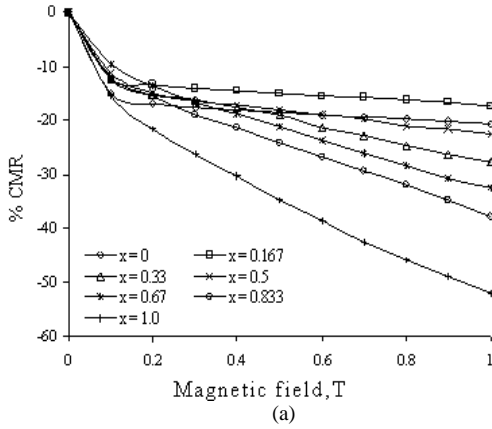
T_0 have been estimated and it is found to increase with increasing the concentration of Nd. From Eq. 2 we also estimated $N(E_F)$ (Table 2). The $N(E_F)$ value for the present sample is found to be decreasing with the application the concentration of Nd.

$\theta_D/2$ values are also estimated, based on the graph $\theta_D/2 \approx T^{-1/4}$ where deviation from linearity occurs in the temperature region above T_p . The θ_D values are found to decrease systematically with increasing Nd

concentration (Table 2). ν_{ph} (the optical phonon frequency) was obtained from the relation of ($h\nu_{ph} = K_B\theta_D$). The values of phonon frequency and $\theta_D/2$ decreased against concentration. These indicate that the frequency of lattice wave decrease with increasing the Nd content. As the concentration of Nd increase, the vibrational energy in periodic solids decreased. It seems that the values of $\theta_D/2$ is much

higher than T_p which shows the width of VRH region between $\theta_D/2$ and T_p .

Magnetoresistance: The corresponding MR ratio is also performed in Fig. 4. The MR ratio is calculated according to $MR (\%) = [(\rho(0)-\rho(H))/\rho(0)] \times 100\%$, where $\rho(0)$ is the zero field resistivity and $\rho(H)$ is the resistivity with magnetic field of $H = 1T$. Over all,



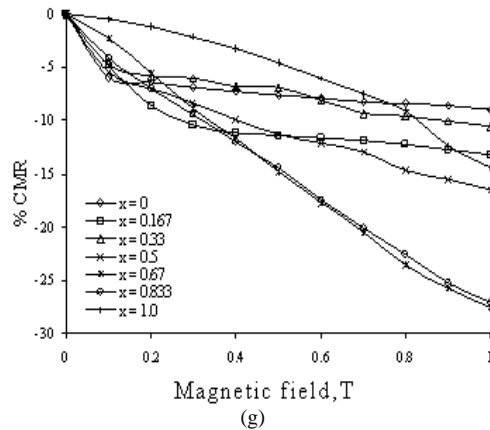


Fig. 4: CMR curve of $(La_{1-x}Nd_x)_{0.5}Ba_{0.5}MnO_3$ system as a function of applied magnetic field at 300 K. (a): 90 K; (b): 100 K; (c): 150 K; (d): 200 K; (e): 250 K; (f): 270 K and (g): 300 K

Table 2: Values of the Density Of States (DOS) at Fermi level $N(E_F)$, activation Energies (E_a), $\theta_D/2$ and phonon frequency, ν (Hz) and from resistivity

x	T_p (K)	T_0	$N(E_F)$ ($eV^{-1}cm^{-3}$) $\times 10^{22}$	$\theta_D/2$	ν (Hz) $\times 10^{12}$
0.00	252	45.5571	5020.00	-	-
0.167	244	50.0189	4570.00	278.00	5.79
0.330	218	95.4529	2390.00	246.01	5.13
0.500	198	1250.3060	183.000	235.99	4.92
0.670	146	4957.1740	46.1000	190.02	3.96
0.833	130	15422.8400	14.8000	164.00	3.42
1.000	114	192414.8000	1.19000	99.960	2.08

the MR decreases with increasing doping concentration and increases with decreasing temperature. This is due to enhanced inter-grain tunneling magnetoresistance at low temperatures, arising as a result of varying Mn environment at the interfaces. Figure 4 also shows the MR of granular systems consists of Low-Field Magnetoresistance (LFMR) and High-Field Magnetoresistance (HFMR), which are closely related to the surface effects of the grains. The region of Low-Field Magnetoresistance (LFMR) is considering from 0T to 0.1T, while the region of Low-Field Magnetoresistance (LFMR) is considering from 0.1T-1T. Figure 4c-f shows that the existing of LFMR. At low field (about 0.1T), the gradient of MR is 154.71% MR/Tesla, observed at 90 K for $x = 1.0$. For high field (0.1-1T), the field gradient of MR value is about 40.68% MR/Tesla. Normal negative CMR effect with non saturation condition had been observed. These show that higher (more than 1 Tesla) magnetic field is needed to fully reorient its magnetic spin. Low concentration of doping ($0.0 \leq x \leq 0.5$) give two regions of MR effect significantly, which is low field (0.0-0.1 Tesla) and high field (0.1-1 Tesla) magnetoresistance. However, at concentration of $x \geq 0.67$, linear relationship is observed.

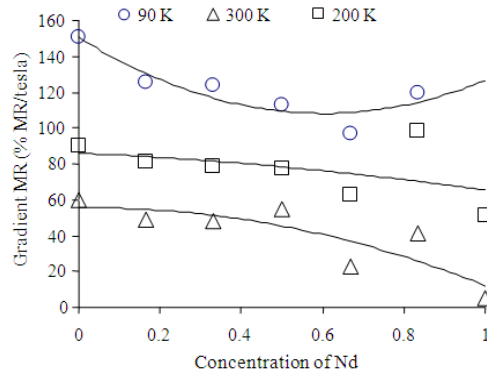


Fig. 5: Plot of % LFMR as function of Nd concentration

Figure 5 shows the plot of the gradient MR against concentration. This can be seen that the highest field gradient of MR can be obtained by samples measured at 90K. At this temperature, samples give a large variation of LFMR in range, ~100~160% MR/Tesla. These values are very sensitive for low field application and therefore it's also acceptable as a requirement for a sensing element.

Overall, MR drops slowly when temperature rises as shown in Fig. 6. All doping concentration gives small variation range (~10~63.43%). The highest MR value of 63.43% is observed at 150 K for sample of $x = 1.0$, near the MI transition temperature. Samples exhibit highest MR values close to their T_p values. Close to T_p , the enhancements of MR are caused by the change of magnetic ordering from spin disorder of paramagnetic ordering to order spin of ferromagnetism ordering. Thus, the spin disorder scattering induced by a long range hopping correlation and its fluctuation, which is the possible origin of the CMR phenomena in doped manganites, is reduced.

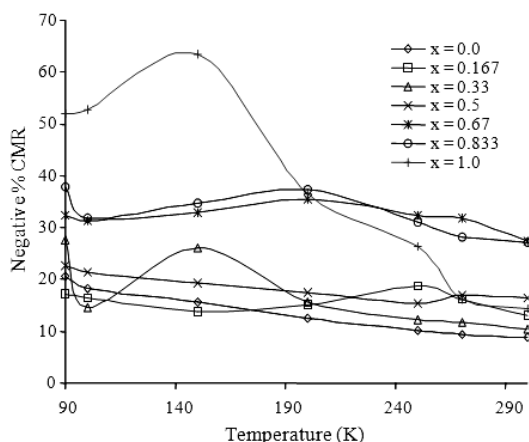


Fig. 6: %MR of $(\text{La}_{1-x}\text{Nd}_x)_{0.5}\text{Ba}_{0.5}\text{MnO}_3$ systems as function of temperature dependent

Within a single magnetic domain, the e_g electrons transfer between Mn^{3+} and Mn^{4+} ions is easy. The pairs of Mn^{3+} and Mn^{4+} spins, which may not be parallel in the vicinity of domain wall boundaries, will act as a hindrance for electron transport. The magnetic domains tend to align along the field direction in the presence of sufficiently strong magnetic field. As a result, hopping of electrons become easy across the domain wall boundaries and the resistivity decreases, which in turn leads to significant MR at low temperature.

CONCLUSION

The electrical and magnetoresistive properties of trivalent Nd doping in La-Ba-Mn-O systems drives the system towards lower conductivity and lower metal-insulator transition temperature region. It has been found that the electrical conduction mechanism of these materials at low temperatures ($T < T_p$) may be due to electron-electron and two magnon scattering processes, while in the high temperature regime ($T > T_p$) the conduction is due to variable range mechanism. The non-saturating MR value at low temperatures is observed in the case of $x = 0.5, 0.67, 0.833$ and 1.0 . In addition, sample $x = 1.0$ exhibits a very high MR ($\sim 63.43\%$) at 1 tesla measured at 150 K. At 90 K, samples give a large variation of LFMR in range, $\sim 100\text{--}160\%$ MR/Tesla. These values are very sensitive for low field application and therefore it's also acceptable as a requirement for a sensing element

ACKNOWLEDGEMENT

The Ministry of Science, Technology and Innovation of Malaysia is gratefully acknowledged for the grant under IRPA vote: 03-02-04-0374-SR0003/07-07.

REFERENCES

1. Abdelmoula, N., A. Cheikh-Rouhou and L. Reversat, 2001. Structural, magnetic and magnetoresistive properties of $\text{La}_{0.7}\text{Sr}_{0.3-x}\text{Na}_x\text{MnO}_3$ manganites. *J. Phys. Condens. Matter*, 13: 449-458. DOI: 10.1088/0953-8984/13/3/307
2. Subramaniam, M.A., B.H. Toby, A.P. Ramirez, W.J. Marshall, A.W. Sleight and G.H. Kwei, 1996. Colossal magnetoresistance without $\text{Mn}^{3+}/\text{Mn}^{4+}$ double exchange in the stoichiometric pyrochlore $\text{Ti}_2\text{Mn}_2\text{O}_7$. *Science*, 273: 81-84. DOI: 10.1126/science.273.5271.81
3. Radaelli, P.G., D.E. Cox, M. Marezio, S.W. Cheong, P.E. Scifferm and A.P. Ramirez, 1995. Simultaneous structural, magnetic and electronic transitions in $\text{La}_{1-x}\text{Ca}_x\text{MnO}_3$ with $x=0.25$ and 0.50 . *Phys. Rev. Lett.*, 75: 4488-4491. DOI: 10.1103/PhysRevLett.75.4488
4. Sayani, B., S. Pal, R.K. Mukherjee and B.K. Chaudhuri, 2004. Development of pulsed magnetic field and study of magnetotransport properties of K-doped $\text{La}_{1-x}\text{Ca}_x\text{K}_y\text{MnO}_3$ CMR materials. *J. Magn. Magn. Mater.*, 269: 359-371. DOI: 10.1016/S0304-8853(03)00632-2
5. Ziese, M., 2000. Spontaneous resistivity anisotropy and band structure of $\text{La}_{0.7}\text{Ca}_{0.3}\text{MnO}_3$ and Fe_3O_4 films. *Phys. Rev.*, B 62: 1044. DOI: 10.1103/PhysRevB.62.1044
6. Mott, N.F., 1990. *Metal-Insulator Transition*. 2nd Edn., Chapter 9, Taylor and Francis, London.
7. Zener, C., 1951. Interaction between the d-shells in the transition metals. II. Ferromagnetic compounds of manganese with perovskite structure. *Phys. Rev.*, 82: 403-405. DOI: 10.1103/PhysRev.82.403
8. Asthana, S., D. Bahadur, A.K. Nigam and S.K. Malik, 2004. Magneto-transport studies on $(\text{Pr}_{1/3}\text{Sm}_{2/3})_{2/3}\text{A}_{1/3}\text{MnO}_3$ ($A = \text{Ca}, \text{Sr}$ and Ba) compounds. *J. Phys. Condens. Matter*, 16: 5297-5307. DOI: 10.1088/0953-8984/16/29/020